Liquid phase oxidation of alkanes using Cu/Co-perchlorophthalocyanine immobilized MCM-41 under mild reaction conditions

P. Karandikar, A.J. Chandwadkar [*], M. Agashe, N.S. Ramgir, S. Sivasanker

Catalysis Division, National Chemical Laboratory, Pune 411008, India

Abstract

Amino-functionalized MCM-41 (NH$_2$-MCM-41) was used to immobilize Cu/Co-Cl$_{16}$Pc complex, i.e. Cu/Co-AM(PS) for liquid phase oxidation of alkanes under mild reaction conditions. Higher rates of reaction and better catalytic activity values were obtained for Cu/Co-AM(PS) as compared to Cu/Co-Cl$_{16}$Pc grafted on (i) amino-functionalized SiO$_2$ [Cu/Co-ASiO$_2$] and (ii) non-functionalized MCM-41 [Cu/Co-M(I)] catalysts along with neat metal complex under identical conditions. The catalysts were evaluated by comparing two different oxidants: (i) TBHP and (ii) O$_2$/aldehyde. The rate of conversion and percent selectivity differ for the above two oxidants due to differences in stability of radical species and in their homolytic/heterolytic pathways. The homolytic dissociation of oxygen favors a higher rate of conversion in the case of TBHP, whereas the heterolytic mechanism favors a higher selectivity for cyclohexanone in the case of O$_2$/aldehyde. The catalysts were characterized by XRD, MAS NMR, N$_2$-adsorption, microanalysis, UV–vis, FTIR and cyclic voltammetry. The UV–vis spectra reveal a blue shift for the metal phthalocyanine-immobilized samples, indicating unimolecular dispersion of metal complex within the channels of MCM-41. Cyclic voltammetry results suggest some coordinative interaction of the amino group of NH$_2$-MCM-41 with the metal on grafting with the complex.
© 2005 Elsevier B.V. All rights reserved.

Keywords: MCM-41; Immobilization; Dispersion; Cu/Co-AM(PS); Alkane oxidation; Axo-metal species

1. Introduction

The catalytic conversion of alkanes directly to alcohols using molecular oxygen has become increasingly important as a means of converting these easily available and inexpensive hydrocarbons to valuable chemical and fuel products. A number of biological systems including cytochrome P-450 and methane mono-oxygenase are known to convert alkanes to alcohols [1]. An increasing understanding of the enzymes together with the growing need for catalysts that can activate aliphatic C–H bonds for selective oxidation has initiated activity to mimic biological systems with synthetic or biomimetic analogs. Transition metal complexes, especially metallophthalocyanines, immobilized in the molecular sieve cavities have become of interest, because they combine the advantages of homogeneous and heterogeneous catalytic systems. An electric field present inside the inorganic matrix is believed to improve the activity, stability, selectivity and life of the catalyst [2].

Many attempts have been made to oxidize alkanes, especially cyclohexane, under mild conditions using different oxidants, such as hydrogen peroxide, ter-butyl hydroperoxide and molecular oxygen [3]. Metal phthalocyanines (MPCs) are cheap and effective selective oxidation catalysts [4]. In the solid state and in some solutions, the complexes are in an 'associative state' and are not very effective as catalysts. To achieve complete dispersion, many authors have encapsulated these complexes inside the cages of zeolites, such as X and Y. The selective oxidation of cyclohexane to cyclohexanol, cyclohexanone and adipic acid at near ambient conditions has been reported over zeolite X and zeolite Y encapsulated phthalocyanines of Fe, Cu and Co. An increase in TON and significant differences in activity and selectivity were observed when compared to the neat complexes [5]. The major disadvantage of these encapsulated complexes is that the zeolite pores are narrow (0.74 nm) and little space is available inside the cages for the substrates to undergo reaction. There is, therefore, an obvious benefit in using large pore material to disperse the complexes. A series of Cu^{2+}-phthalocyanines and Co^{2+}-perfluorophthalocyanines have been prepared inside the pores of MCM-41 using *o*-dicyanobenzene. Here, CoF$_{16}$PcMCM-41 was found to be more active and

---
* Corresponding author. Tel.: +91 20 25893400; fax: +91 20 25893761.
E-mail address: aj.chandwadkar@ncl.res.in (A.J. Chandwadkar).

selective than $CoF_{16}PcY$ for cyclohexane oxidation using TBHP [6]. Industrially, the aerobic oxidation of cyclohexane to cyclohexanol and cyclohexanone is carried out in the liquid phase using homogeneous Co-catalysts with rather low yields of the alcohol and ketone [7].

Recently, Guo et al. [8] have studied cyclohexane oxidation using Co, Fe and Mn tetraphenyl porphyrins as catalysts in homogenous conditions. Molecular oxygen at ~0.6 MPa was used as an oxidant in the absence of additives. Mesoporous (Cr) MCM-41 samples with different chromium contents were prepared hydrothermally and their activities in cyclohexane oxidation were compared with those of different chromium containing molecular sieves (AlPO-5, zeolite β and silicalite-1) [9].

Komiya et al. have discussed the role of different aldehydes in the oxidation of various alkanes and alkenes using copper salts, copper–crown ether complex and a mixture of copper salt and crown ether [10]. Iron and ruthenium-catalyzed oxidation of alkanes with aerobic oxygen in the presence of aldehydes was studied by Murahashi et al. [11]. The peracids formed in the reaction further react with the metal species to afford the metal-oxo species. In an earlier study, we compared two oxidizing agents, namely alkyl hydroperoxide (TBHP) and O_2/isobutyraldehyde, for olefin oxidation using $CuCl_{16}Pc$-immobilized MCM-41 under mild conditions [12]. The O_2/aldehyde oxidant gave more than two times higher conversion and epoxide selectivity than TBHP due to predominant formation of the oxo-metal species.

The main objective of this research is to investigate the use of metal-PCs tethered inside the pores of large pore material as selective oxidation catalysts for some model substrates using two different oxidants. In the present work, the catalysts were prepared by: (i) grafting/immobilization/anchoring of metal complexes (Cu/Co-$Cl_{16}Pc$) on the surface of amino-modified MCM-41 [Cu/Co-AM(PS)], (ii) impregnation within the pores of MCM-41 [Cu/Co-M(I)] and (iii) anchoring on the surface of amine-modified SiO_2 [Cu/Co-ASiO_2]. The activities of the above supported complexes were compared with those of neat metal complexes in the oxidation of alkanes (cyclic and straight chain alkanes) under mild reaction conditions (298 and 323 K) using different oxidants.

2. Experimental

2.1. Materials

Fumed silica (99% pure), cetyltrimethylammoniumbromide (CTMABr, 98% pure), tetramethylammoniumhydroxide (TMA hydroxide, 99% pure), copper/cobalt-perchlorophthalocyanine (Cu/Co$Cl_{16}Pc$, 99% pure) and 3-aminopropyl-triethoxysilane (3-APTES, 99% pure) were purchased from Aldrich. Tetramethylammoniumsilicate (TMA silicate, 10 wt% silica solution) was purchased from SACHEM Inc., USA. Ammonium hydroxide (25% solution in water) was purchased from S.D. Fine Chem. Ltd. Solvents like acetone, acetonitrile, chloroform and toluene (all A.R. grade) were

purchased from E. Merck India Ltd.; all were distilled and dried before use.

2.2. Preparations

MCM-41 was synthesized and characterized according to the published procedure [13]. The molar composition of the synthesis gel in terms of oxides was as follows: SiO_2:0.086 $(NH_4)_2O$:0.089 $(CTMA)_2O$:0.155 $(TMA)_2O$:40 H_2O. Cu/Co-$Cl_{16}Pc$ complex was immobilized on the surface of Si-MCM-41 by two methods: (i) grafting/anchoring on the 3-aminopropyl-triethoxysilane modified MCM-41, i.e. [Cu/Co-AM(PS)] and (ii) impregnating/immobilizing directly on MCM-41, i.e. [Cu/Co-M(I)] following our earlier reported procedure for immobilization of $CuCl_{16}Pc$ on MCM-41 [12]. Grafting/anchoring of Cu/Co-$Cl_{16}Pc$ has been done on the 3-aminopropyltriethoxysilane modified SiO_2, i.e. [Cu/Co-ASiO_2] under similar conditions and results are compared.

2.3. Catalyst characterization

Crystalline phase identification of as-synthesized, calcined and modified samples was carried out by XRD (Rigaku; Miniflex) using nickel-filtered Cu Kα radiation. The solid-state magic-angle spinning (MAS) NMR spectroscopy studies were carried out on a Bruker MSL-500 FT-NMR spectrometer. The chemical compositions of the samples were determined by a combination of wet chemical methods, atomic absorption spectroscopy (Hitachi, Model 2800) and elemental analysis (Carlo Erba; EA1108). The surface area and pore volume were determined from N_2 adsorption isotherms using a Coulter (Omnisorb, 100 CX) instrument. The UV–vis spectra were recorded using a nujol mull on a SHIMADZU, UV-2101 PC spectrometer. The infrared spectra were recorded using fluorolube mull on SHIMADZU-8300 FTIR spectrophotometer. Cyclic voltammetry was carried out using a sample-coated Pt electrode (500 μm radius) and 0.1 M KNO_3 in DMSO with SCE as the reference electrode. The experiments were performed on an Autolab PGSTAT 30 (ECO CHEMIE) electrochemical analyzer using GPES software. The solutions were purged with pure argon for 30 min prior to the analysis.

2.4. Catalytic reaction

Cyclohexane (99%), *n*-decane (99%), acetonitrile (99%), TBHP in decane (5.5 M), TBHP in EDC (30% solution), isobutyraldehyde (98%) and benzaldehyde (98%) were used as reactants without further purification. Catalytic reactions were carried out according to the following procedure. Substrate, solvent and catalyst were first introduced into a round-bottom flask. After the addition of oxidant, the reaction was started by immersing the flask in to the oil bath kept at the reaction temperature. The reaction was carried out with vigorous stirring. All the products were quantified at different intervals by gas chromatography: Chrompack CP900 (Carbowax 20 M); 50 m × 0.32 mm capillary column, using toluene as an internal standard.

3. Results and discussion

3.1. X-ray powder diffraction

X-ray diffraction (XRD) of MCM-41 revealed a typical four-peak pattern [14] with a strong (1 0 0) reflection at $2\theta = 2.4°$ and three weak (1 1 0), (2 0 0) and (2 1 0) reflections at $2\theta = 3.8–5.8°$ arising from the quasi-regular arrangement of mesopores with hexagonal symmetry. The XRD patterns of Co-AM(PS) and Co-M(I) were identical to that of MCM-41, indicating that the structure of MCM-41 was intact in the catalyst samples. A similar observation was made by us earlier when $CuCl_{16}Pc$ was grafted in the channels of MCM-41 [12].

3.2. Solid state MAS NMR spectroscopy

The interaction of 3-APTES with Si-MCM-41 was confirmed by the decrease of the silanol signals Q_2 (−91.6 ppm) and Q_3 (−101.5 ppm) and the appearance of a signal characteristic of $(SiO)_3Si-CH_3$ group (−68.22 ppm) in the ^{29}Si MAS NMR spectrum. CP MAS NMR of NH_2-MCM-41 revealed amino-propyl carbon signals at 6.4, 18.1 and 39.2 ppm. These observations indicate that 3-APTES reacted with the hydroxyl groups on the walls of Si-MCM-41 [4].

3.3. Physicochemical analysis

The physicochemical properties of the samples are presented in Table 1. The surface area of MCM-41 decreases substantially on loading of 3-APTES. Further decrease in the surface area due to loading of the metal complex for [Cu/Co-AM(PS)] is relatively smaller. A large surface area loss is also observed when $Cu/Co-Cl_{16}Pc$ is loaded by impregnation (Table 1). The large surface area loss during the deposition of 3-APTES and impregnation of the metal complex may be attributed to deposition of the molecules inside the pores.

The carbon and nitrogen contents in the sample are presented in Table 1. The experimentally observed C/N (wt%) ratio of 3.0 for the NH_2-MCM-41 sample is close to the expected value of 2.6. Assuming that all the carbon found in the 3-APTES treated samples comes from the aminopropyl group, calculations suggest that about one aminopropyl group is present for every 15 Si. Similarly, if we assume that the

additional carbon present in the Cu-Pc loaded sample [Cu-AM(PS)] comes from the $CuCl_{16}Pc$ molecules, then the number of phthalocyanine molecules present is approximately one for about 500 Si. The ratio of MPc/amino group is nearly 46. Additionally, calculations reveal that, for a monolayer coverage of $CuCl_{16}Pc$ molecules on the surface of NH_2-MCM-41, the copper percentage should be ~3 wt%. This is about 15 times larger than the copper content (0.2 wt%) of Cu-AM(PS), suggesting that only about 6% of the surface is actually covered by phthalocyanine molecules. Similar calculations are also valid for Co-AM(PS). The calculations suggest that the $MCl_{16}Pc$ molecules (M = Cu/Co) are well dispersed on the surface of MCM-41. It is likely that the complexes are attached to the surface through an interaction of the metal atom with the $–NH_2$ group of NH_2-MCM-41 (discussed later).

3.4. Electronic spectroscopy

The UV–vis electronic spectra of $Cu/Co-Cl_{16}Pc$, Cu/Co-M(I), NH_2-MCM-41 and Cu/Co-AM(PS) were recorded using nujol mulls (Fig. 1(A and B)). The UV–vis spectra of NH_2-MCM-41 do not have any absorption band in the region 250–800 nm. Cu/Co-AM(PS), Cu/Co-M(I) and $Cu/Co-Cl_{16}Pc$ (Fig. 1(A and B), curves 1–3, respectively) exhibit strong absorption bands with a maximum at ~300 nm and in the region of 550–800 nm due to ligand $\pi–\pi^*$ electronic transitions. The maximum position of the broad band of $CoCl_{16}Pc$ is shifted from ~652 to 637 nm on anchoring the complex with the 3-APTES-modified MCM-41, [Co-AM(PS)]. Similarly, the band maximum of $CuCl_{16}Pc$ is also shifted from ~654 to ~643 nm for Cu-AM(PS). This blue shift is indicative of an increased π overlap on immobilization/grafting of the complex molecule. In contrast to this, Balkus et al. [15] observed a red shift on encapsulation of $Cu/Co-F_{16}Pc$ in NaX zeolites and attributed it to a distortion of the phthalocyanine ligands in zeolite cages.

3.5. Infrared spectroscopy

The mid-infrared region from 1300 to 400 cm^{-1} was recorded using nujol mull. The IR spectra due to lattice vibrations of as-synthesized and calcined Si-MCM-41

Table 1
Physicochemical properties of the samples

Sample	C/N analysis (wt%)		S_{BET} (m²/g)	Pore volume (ml/g)	Pore diameter (Å)
	C	N			
$CuCl_{16}Pc$	33.86	9.94	57	–	–
Si-MCM-41	–	–	1115	0.65	38
NH_2-MCM-41	4.17	1.39	569	0.24	26
Cu-M(I) (0.2)[a]	1.43	0.33	421	0.32	29
Cu-AM(PS) (0.2)[a]	6.00	1.42	384	0.22	25
$CoC_{16}Pc$	34.00	9.00	54	–	–
Co-M(I) (0.2)[a]	1.43	0.33	450	0.34	30
Co-AM(PS) (0.2)[a]	6.05	1.43	412	0.24	26

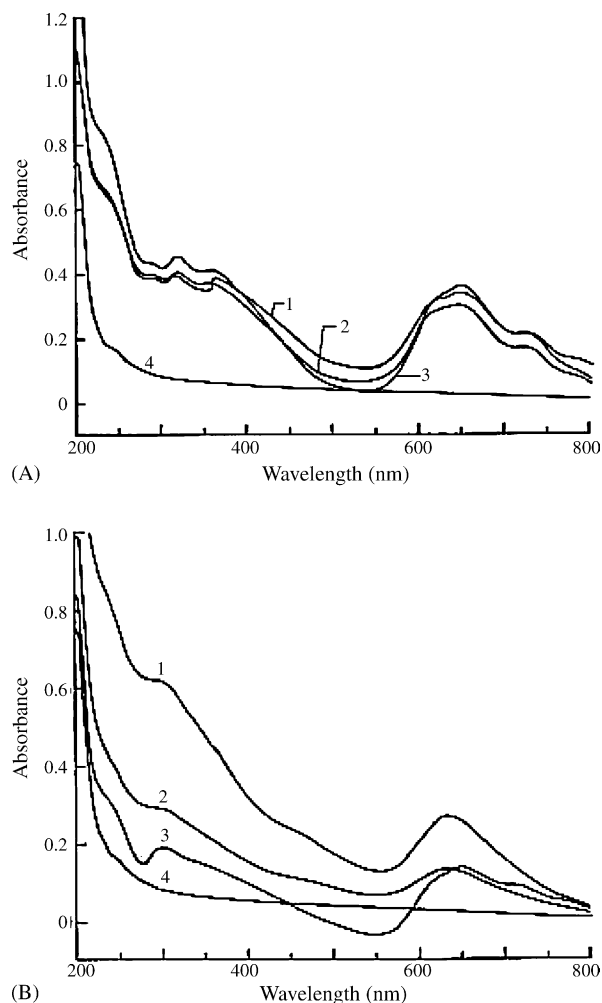[a] Amount of Cu/Co present in the catalyst (from AAS analysis).

Fig. 1. UV–vis spectra of (A) 1, Cu-AM(PS); 2, Cu-M(I); 3, CuCl$_{16}$Pc; 4, NH$_2$-MCM-41 and (B) 1, Co-AM(PS); 2, Co-M(I); 3, CoCl$_{16}$Pc; 4, NH$_2$-MCM-41.

molecular sieves revealed series of bands characteristic of SiO$_4$ tetrahedral unit assigned to asymmetric and symmetric stretching and deformation modes (Fig. 2(A) inset). The band observed at~1085 cm^{-1} is characteristic of mesoporous molecular sieves [12]. The IR spectra (2000–1300 cm^{-1}) of the original and grafted/modified samples of MCM-41 were recorded (Fig. 2(A)) using flurolube. The presence of a metal phthalocyanine complex in the grafted samples was revealed by a band at ~1390 cm^{-1}. However, the intensity of the band was small compared to that in the neat complex due to the low concentration of the Cu/Co-Cl$_{16}$Pc complex in the Cu/Co-AM(PS) samples (compare curve 2 with curve 3 for copper-containing sample and curve 4 with curve 5 for cobalt-containing samples). The negligible shift of the band position is indicative of the undisturbed planarity of the Cu/Co-Cl$_{16}$Pc complex on incorporation in Si-MCM-41 (effective pore diameter ~28 Å).

The IR spectra (recorded using fluorolube) of Si-MCM-41, NH$_2$-MCM-41 and Cu/Co-AM(PS) in the 4000–1300 cm^{-1} region are presented in Fig. 2(B). The broad band centered at ~3400 cm^{-1} observed in the case of MCM-41 is due to stretching vibrations of adsorbed water and silanol hydroxyl groups. The band at 1630 cm^{-1} is assigned to the deformation vibrations of water.

The spectra of NH$_2$-MCM-41 and Cu/Co-AM(PS) exhibit bands at ~3365 and ~3285 cm^{-1} superimposed on a broad band that can be assigned to asymmetric and symmetric stretching vibrations of amino group. Based on the FTIR spectra of the samples, it is not possible to confirm the interaction of the –NH$_2$ group of NH$_2$-MCM-41 with the central metal atom of Cu/Co-Cl$_{16}$Pc. We have reported earlier that an adduct of *n*-hexylamine with CuCl$_{16}$Pc exhibits a band at 1650 cm^{-1} attributable to –NH$_2$ deformation [12]. However, this band is not observed very clearly in the Cu/Co-AM(PS) samples due to strong absorption by water molecules in that region. Besides, in view of the large number of uncoordinated –NH$_2$ groups on the surface, it is unlikely that any shift in the –NH$_2$ frequency will be easily observed. Therefore, in view of the fact that the metal phthalocyanine complex form adducts with amines and based on earlier reports that –NH$_2$ frequencies were not altered on coordination with Cu–schiff base complexes [16], we believe that interactions between the –NH$_2$ group of NH$_2$-MCM-41 and Cu/Co occurs in the samples.

3.6. Cyclic voltammetry

The electrochemical behavior of the samples was studied by cyclic voltammetry using 0.1 M KNO$_3$ in DMSO (dimethyl-sulphoxide) solution in the potential range of +0.5 to −2.0 V [17]. The sample-coated Pt wire (500 μm diameter) was the working electrode and a Pt wire was used as the counter electrode. A standard calomel electrode (SCE) was used as the supporting electrode. The electrolyte solution was purged with argon prior to the analysis.

The CoCl$_{16}$Pc catalysts reveal an initial central metal redox process followed by a ring reduction process, whereas in the case of CuCl$_{16}$Pc, the central metal redox process is not observed until the phthalocyanine ring undergoes a redox cycle [18].

When cyclic voltammograms of different catalysts, i.e. Co-ASiC$_2$, Co-M(I) and Co-AM(PS) along with that of the neat metal complex CoCl$_{16}$Pc were recorded, we observed two redox processes: process I for the metal-based electron transfer, Co(II)/Co(I), followed by process II for phthalocyanine ring reduction, [Co(I)Cl$_{16}$Pc(−2)]$^-$/[Co(I)Cl$_{16}$Pc(−3)]$^{-2}$ (Table 2). One can see that for the neat metal complex, the Co(II)/Co(I) redox process is not well defined as a result of slow electron transfer kinetics, which encourages the spontaneous aggrega-

Table 2
Summary of E_{eq} (V/SCE) potential values of redox process

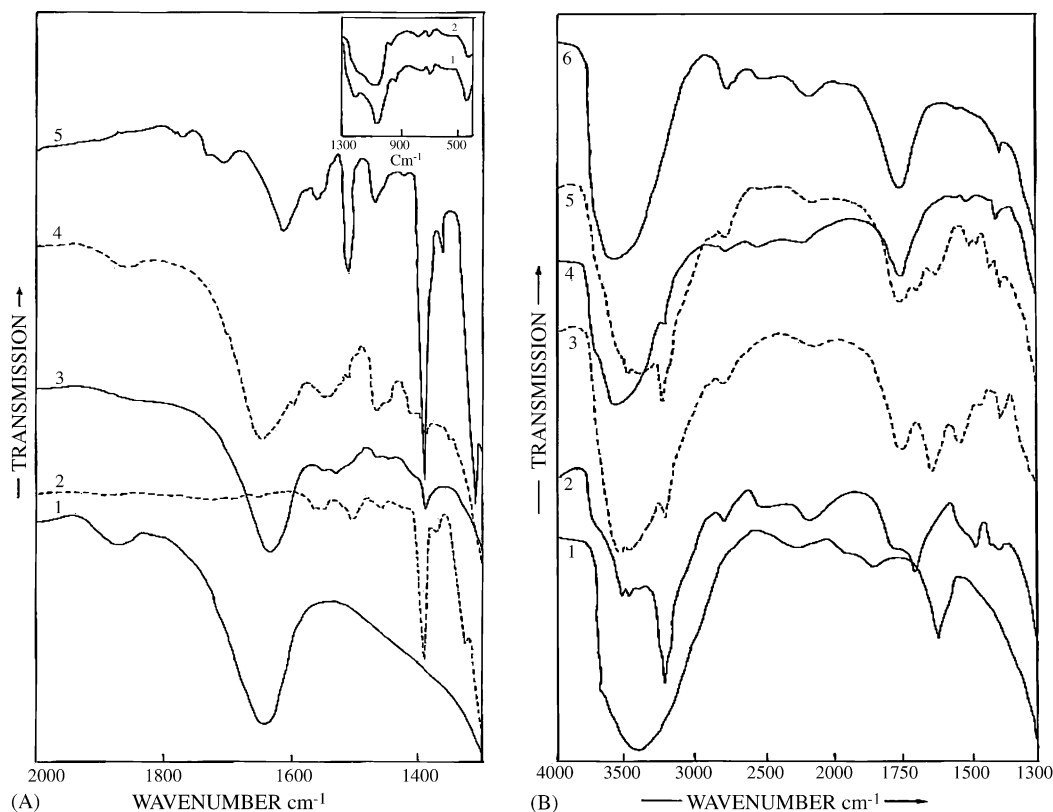| Catalyst	Process I (V)	Process II (V)	Process III (V)
CuCl$_{16}$Pc	–	−0.750	−1.280
Cu-M(I)	−0.337	−0.813	−1.225
Cu-AM(PS)	−0.250	−0.785	−1.275
CoCl$_{16}$Pc	−0.267	−1.105	–
Co-M(I)	−0.260	−1.160	–
Co-AM(PS)	−0.220	−1.155	–

Fig. 2. FTIR spectra of: (A) 1, Si-MCM-41; 2, CuCl$_{16}$Pc; 3, Cu-AM(PS); 4, Co-AM(PS); 5, CoCl$_{16}$Pc (*Inset*: 1, as synthesized Si-MCM-41 and 2, calcined Si-MCM-41). (B) 1, Si-MCM-41; 2, NH$_2$-MCM-41; 3, Cu-AM(PS); 4, Cu-M(I); 5, Co-AM(PS); 6, Co-M(I).

tion of the complex. These redox processes are in agreement with those reported for the CoF$_{16}$Pc complex by Balkus et al. [15]. In the case of CoF$_{16}$Pc, the $E_{1/2}$ value shifted to a more positive potential compared to that for CoCl$_{16}$Pc, due to the electronegativity of the substituted fluorine atoms being higher than that of the chlorine atoms in our case.

In the case of the CoCl$_{16}$Pc impregnated complexes [Co-M(I)] and the post-synthesized catalysts [Co-AM(PS)], the Co(II)/Co(I) redox processes are well defined. This may be attributed to site isolation of the metal complex in the channels of MCM-41, which makes the redox process well defined.

For Co-AM(PS), the redox process for the metal shifts to a positive potential ($E_{1/2} = -0.220$ V) which is higher by +0.04 V than that for the impregnated catalyst; Co-M(I) (i.e. $E_{1/2} = -0.260$ V). This could be due to the interaction of the amino group with the four-coordinated CoCl$_{16}$Pc. The axial interaction of the fifth ligand causes the relative destabilization of Co(II) and stabilization of Co(I) state, thereby shifting the redox potential towards the positive side as compared to that for the four-coordinated complex in the impregnated catalyst [19]. No significant change is observed for the redox process II (phthalocyanine ring reduction) in any of the above catalysts.

In the case of neat CuCl$_{16}$Pc we did not get a redox peak for the metal as reported by Balkus et al. for CuF$_{16}$Pc [15]. The last two redox waves in all cyclic voltammograms are attributed to the ligand reduction process (Table 2). For the different CuCl$_{16}$Pc catalysts we could observe the redox process for the metal due to the molecular distribution of complex, avoiding

the aggregation of the metal. Similar to cobalt catalysts, we observe a shift in the redox process I (redox process for the metal) for Cu-AM(PS) by +0.087 V ($E_{1/2} = -0.25$ V) as compared to the impregnated catalyst, Cu-M(I) ($E_{1/2} = -0.337$ V).

3.7. Catalytic studies

Oxidation of alkanes is an important industrial processes for both economic and environmental reasons. Therefore, it is desirable to replace conventional processes that use stoichiometric oxidants with environmentally more benign ones using alkyl hydroperoxides and hydrogen peroxide, but the best of all would be processes that could selectively oxidize hydrocarbons using either dioxygen or air under mild conditions. As reported in our earlier publication [12], anchored copper catalysts were found to be effective for the oxidation of alkenes with molecular oxygen in the presence of an aldehyde. Therefore, it was decided to use immobilized catalysts for the oxidation of alkanes using different aldehydes as co-oxidants.

3.7.1. Oxidation of cyclohexane using Cu/Co-Cl$_{16}$Pc immobilized catalysts

Cyclohexane oxidation was carried out over Cu/Co-Cl$_{16}$Pc immobilized MCM-41 catalysts using TBHP and O$_2$/isobutyraldehyde as oxidizing agents at two different temperatures, 298 and 323 K. Cu-AM(PS) showed the highest conversion of 3.7 and 3.0% for TBHP and O$_2$/isobutyraldehyde, respectively, at
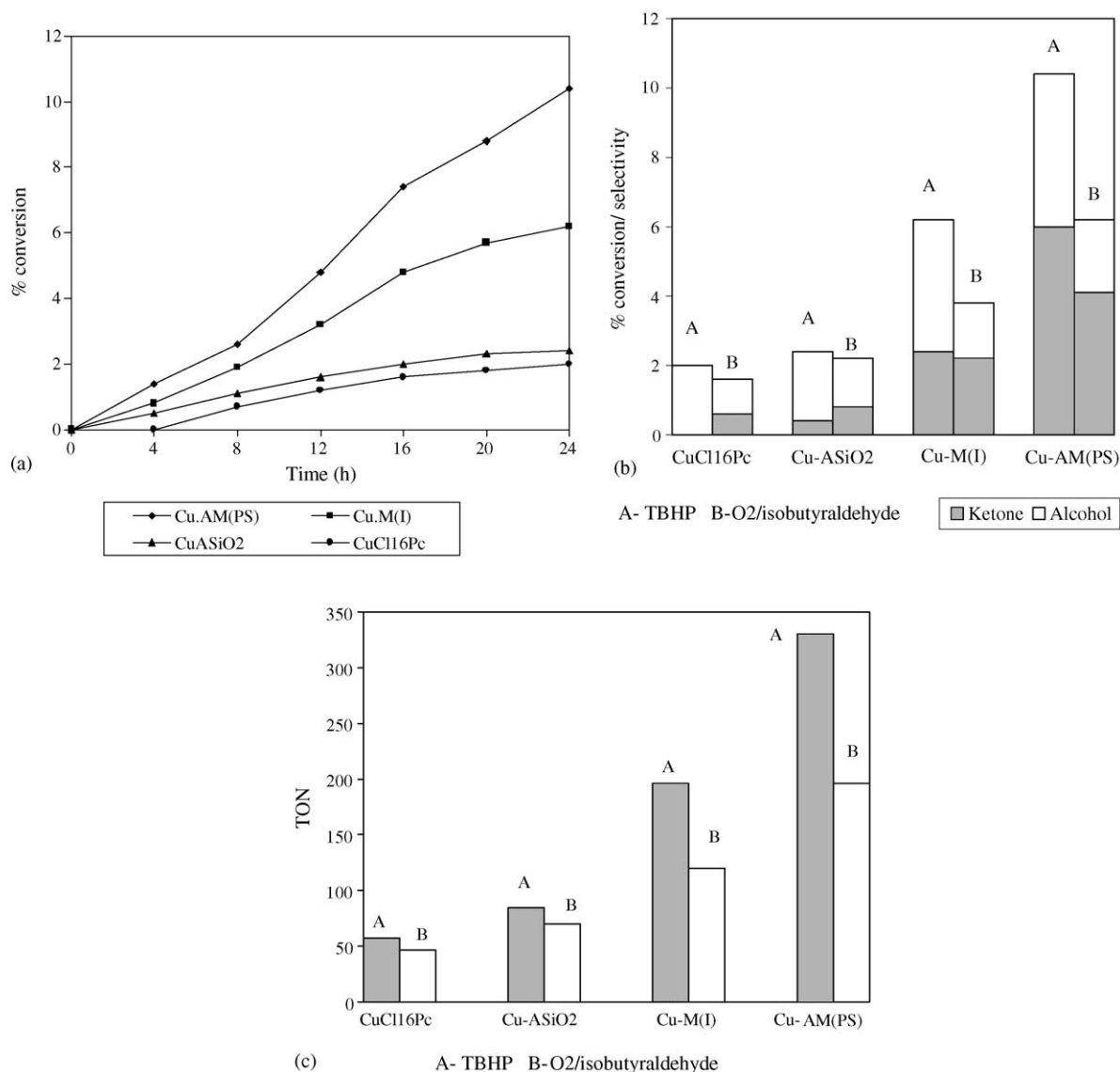
Fig. 3. (a) Kinetic study of cyclohexane oxidation over different $CuCl_{16}Pc$ catalysts using TBHP as oxidant at 323 K. (b) Comparison of (A) TBHP and (B) O_2/isobutyraldehyde for cyclohexane oxidation using different $CuCl_{16}Pc$ catalysts at 323 K. (c) Comparison of TON values for the different $CuCl_{16}Pc$ catalysts: (A) TBHP and (B) O_2/isobutyraldehyde. TON = mole of product formed/mole of metal present in the catalyst/24 h.

298 K in 24 h. Similarly, Co-AM(PS) showed a maximum of 5.1% cyclohexane conversion at 298 K when TBHP was used as the oxidant and 4.4% conversion when O_2/isobutyraldehyde was used as the oxidant.

The kinetic studies at 323 K for both the oxidants (TBHP and O_2/isobutyraldehyde) show that cyclohexane conversion is in the order: $Cu/Co-Cl_{16}Pc < Cu/Co-ASiO_2 < Cu/Co-M(I) < Cu/Co-AM(PS)$ (Figs. 3(a) and 4(a)). TON values at 323 K for the different catalysts using TBHP were: $CuCl_{16}Pc$, 57; $Cu-ASiO_2$, 85; Cu-M(I), 196 and Cu-AM(PS), 330 (Fig. 3(c)). Similarly, TON values at the same temperature for O_2/isobutyraldehyde were: $CuCl_{16}Pc$, 47; $Cu-ASiO_2$, 70; Cu-M(I), 120 and Cu-AM(PS), 196 (Fig. 3(c)). For cobalt-containing catalysts, we observed a similar trend of TON values, the TON value for Co-AM(PS) being the largest compared to other catalysts for both TBHP (TON = 424) and O_2/isobutyraldehyde (TON = 188) (Fig. 4(c)). The high activity of the supported complexes is

due to the large hydrophobic surface area of MCM-41 and to the molecular dispersion of the metal complexes within the pores. Further, the higher conversion of Cu/Co-AM(PS) compared to Cu/Co-M(I) may be due to the anchoring of the metal complex via the amino group to MCM-41, which could enhance the catalytic activity through easy reduction of the metal species [20]. The kinetic plots also show a steady increase in the yields of cyclohexanol and cyclohexanone even at 24 h, specifically in the case of the anchored catalyst. This is due to the inherent stability of the chloro-substituted phthalocyanines, the neutral silica support and the mild conditions of the experiment. Kinetic plots reported earlier for cyclohexane oxidation at an oxygen pressure of 800 psi, using phthlocyanine-anchored catalysts revealed that the conversion was nearly constant after ∼5–8 h [5]. A similar behavior has been observed by Guo et al. [8] for iron/cobalt/manganese tetraphenyl porphyrins immobilized on chitosan at a relatively mild pressure of oxygen 0.6 MPa.
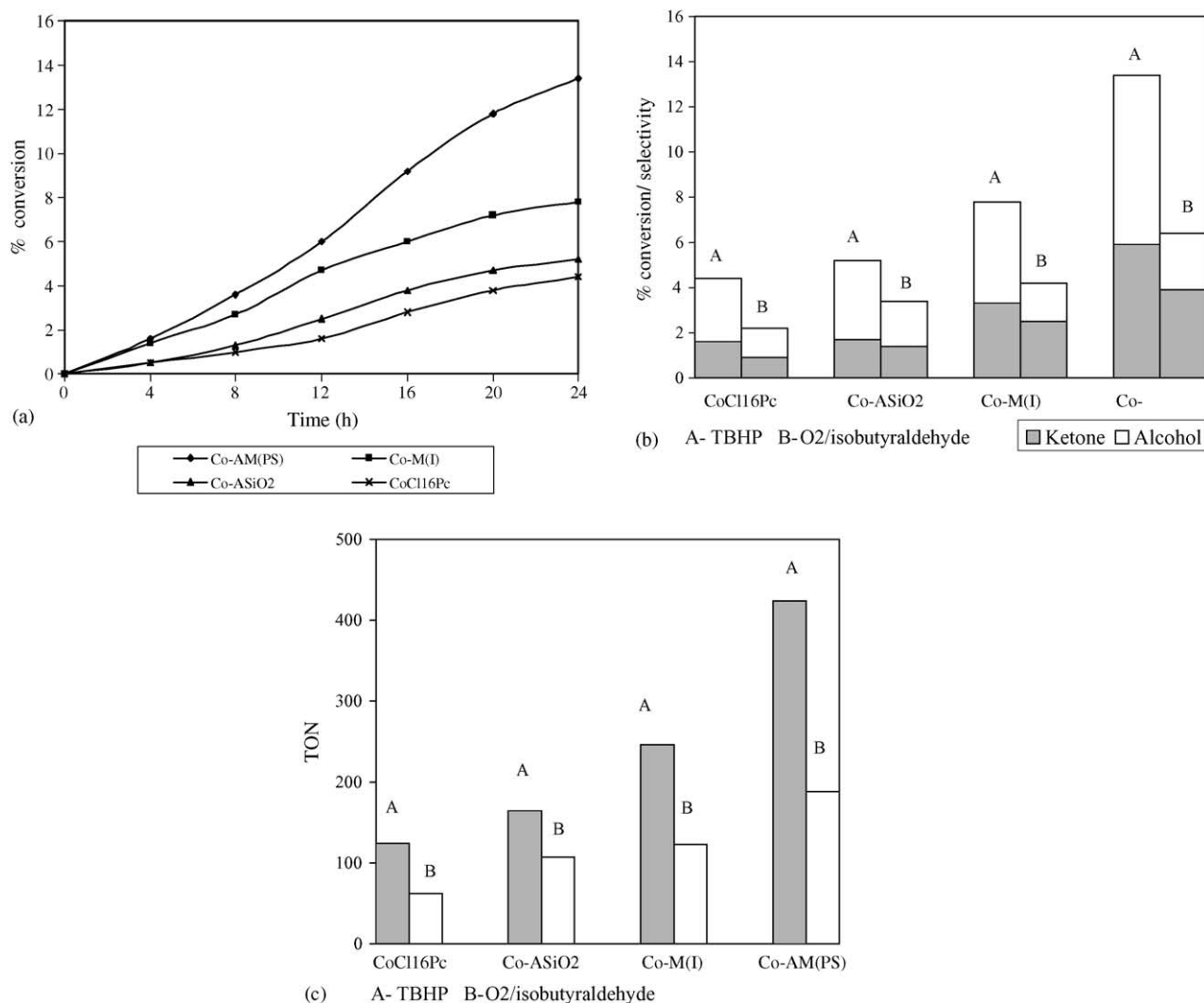
(a)

(b)   A- TBHP   B-O2/isobutyraldehyde   ☐ Ketone ☐ Alcohol

(c)   A- TBHP   B-O2/isobutyraldehyde

Fig. 4. (a) Kinetic study of cyclohexane oxidation using different $CoCl_{16}Pc$ catalysts using TBHP as oxidant at 323 K. (b) Comparison of TBHP and O_2/isobutyraldehyde for cyclohexane oxidation using different $CoCl_{16}Pc$ catalysts at 323 K. (c) Comparison of TON values for the different $CoCl_{16}Pc$ catalysts: (A) TBHP and (B) O_2/isobutyraldehyde. TON = mole of product formation/mole of metal present in the catalyst/24 h.

On comparing the performance of the two oxidizing agents, one will observe that TBHP is nearly two times more active compared to O_2/isobutyraldehyde for cyclohexane oxidation at 323 K (Figs. 3(b) and 4(b)). The conversion is 10.4 and 13.4% for Cu-AM(PS) and Co-AM(PS), respectively, for TBHP, whereas it is 6.2 and 6.4% for O_2/isobutyraldehyde at 24 h. These results are contradictory to our previous reports of olefin oxidation in which exclusive formation of oxo-metal species and heterolytic decomposition were shown to play important roles in enhanced conversion when O_2/isobutyraldehyde was used as the oxidant as compared to TBHP [12].

Alkanes are susceptible to homolytic attacks in which free radicals are intermediates. The [t]BuO radical formed from homolytic decomposition of TBHP, which is more favored than to [t]BuOO [21], preferentially abstracts hydrogen to give the Cy radical. In the case of alkane oxidation, this homolytic decomposition is more favored compared to the heterolytic decomposition of the O–O bond. Also, alkyl peroxy radicals are more stable as compared to acyl peroxy radicals formed by
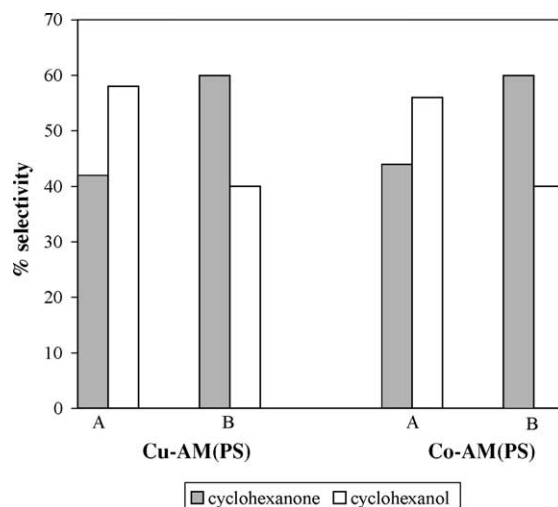

Fig. 5. Comparison of cyclohexanone selectivity for (A) TBHP and (B) O_2/isobutyraldehyde over Cu-AM(PS) and Co-AM(PS) at 323 K.
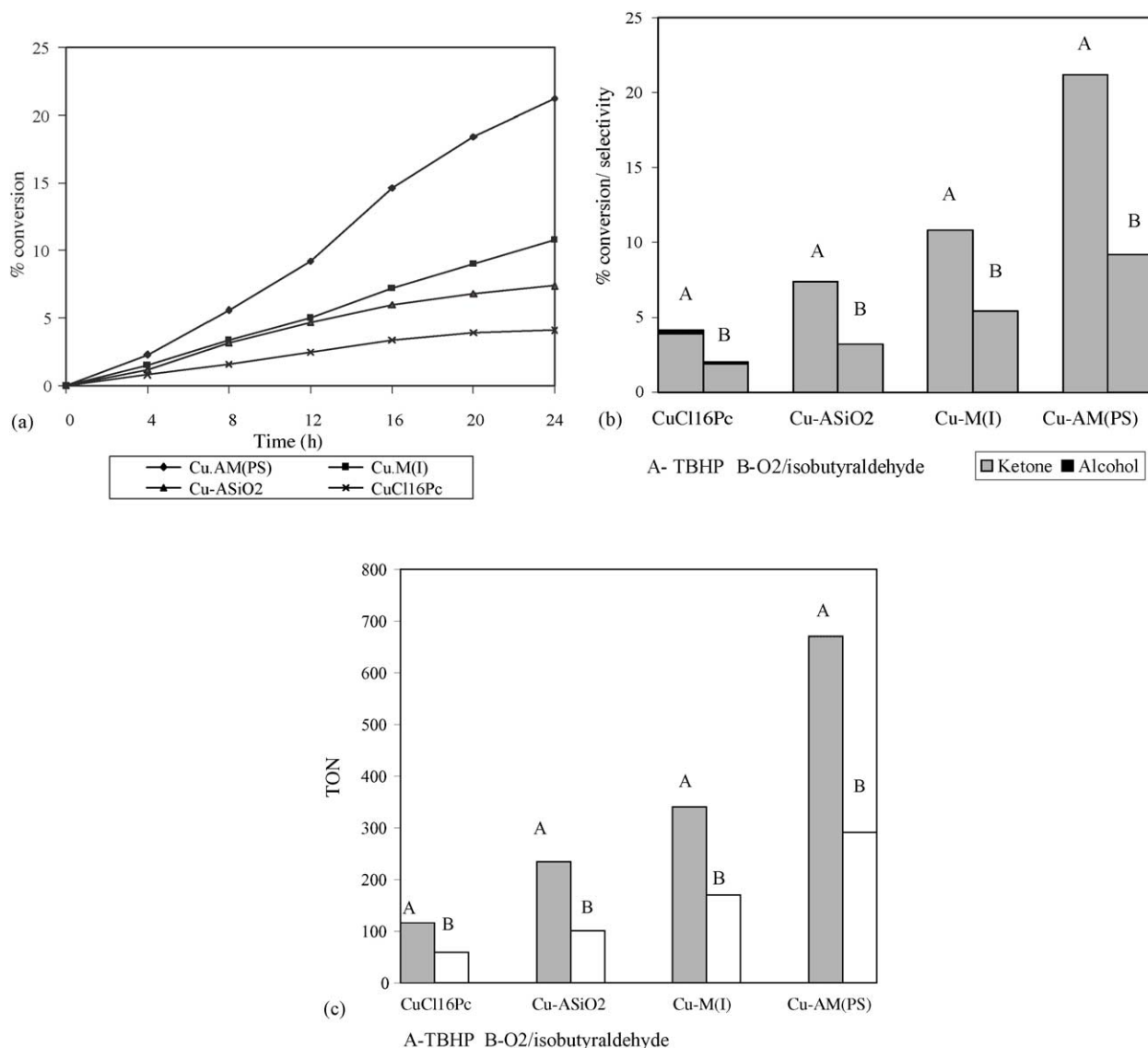
Fig. 6. (a) Kinetic study of *n*-decane oxidation using different $CuCl_{16}Pc$ catalysts using TBHP as oxidant at 323 K. (b) Comparison of TBHP and O_2/isobutyraldehyde for *n*-decane oxidation using different $CuCl_{16}Pc$ catalysts at 323 K. (c) Comparison of TON values for the different $CuCl_{16}Pc$ catalysts: (A) TBHP and (B) O_2/isobutyraldehyde. TON = mole of product formed/mole of metal present in the catalyst/24 h.

isobutyraldehyde that are readily converted into per acids, favoring a heterolytic mechanism. The above arguments may explain the larger alkane oxidation found with TBHP than with O_2/isobutyraldehyde.

The selectivity for cyclohexanone is more for O_2/isobutyraldehyde than for TBHP, the ratio of cyclohexanol:cyclohexanone being 1.0:1.5 for the immobilized catalysts of copper and cobalt, in spite of the low conversions. The interaction of isobutyraldehyde with M^{2+} (where M = Cu or Co) gives an acyl peroxy M^{2+} complex, followed by a heterolytic O–O bond cleavage to give an oxo-metal species [10]. This species abstracts hydrogen to give a cyclohexane radical which reacts with O_2 to produce the cyclohexyl peroxy radical and thus results to a 1.0:1.0 ratio of cyclohexanol and cyclohexanone according to a Russell-type termination reaction [22]. Cyclohexanol is further oxidized simultaneously to give cyclohexanone, which increases the overall ketone yield.

On the contrary, in the case of TBHP, the overall ratio of cyclohexanol:cyclohexanone is 1.5:1.0. The homolysis of the O–O bond in M^{2+}–O–O–^tBu produces ^tBuO, which abstracts a hydrogen atom from cyclohexane to give the corresponding radical species. This species further reacts to give cyclohexanol as the primary product. Fig. 5 presents a comparison of cyclohexanone selectivity between TBHP and O_2/isobutyraldehyde over Cu/Co-AM(PS) catalysts.

3.7.2. Oxidation of n-decane using Cu/Co-$Cl_{16}Pc$ immobilized catalysts

The oxidation of *n*-decane over different Cu/Co-$Cl_{16}Pc$ catalysts was studied at 298 and 323 K using TBHP and O_2/isobutyraldehyde as oxidizing agents. Decane conversion was low for all the Cu/Co-$Cl_{16}Pc$-immobilized MCM-41 catalysts for both the oxidizing agents when the reactions were carried out at room temperature (298 K). It was observed that Cu-
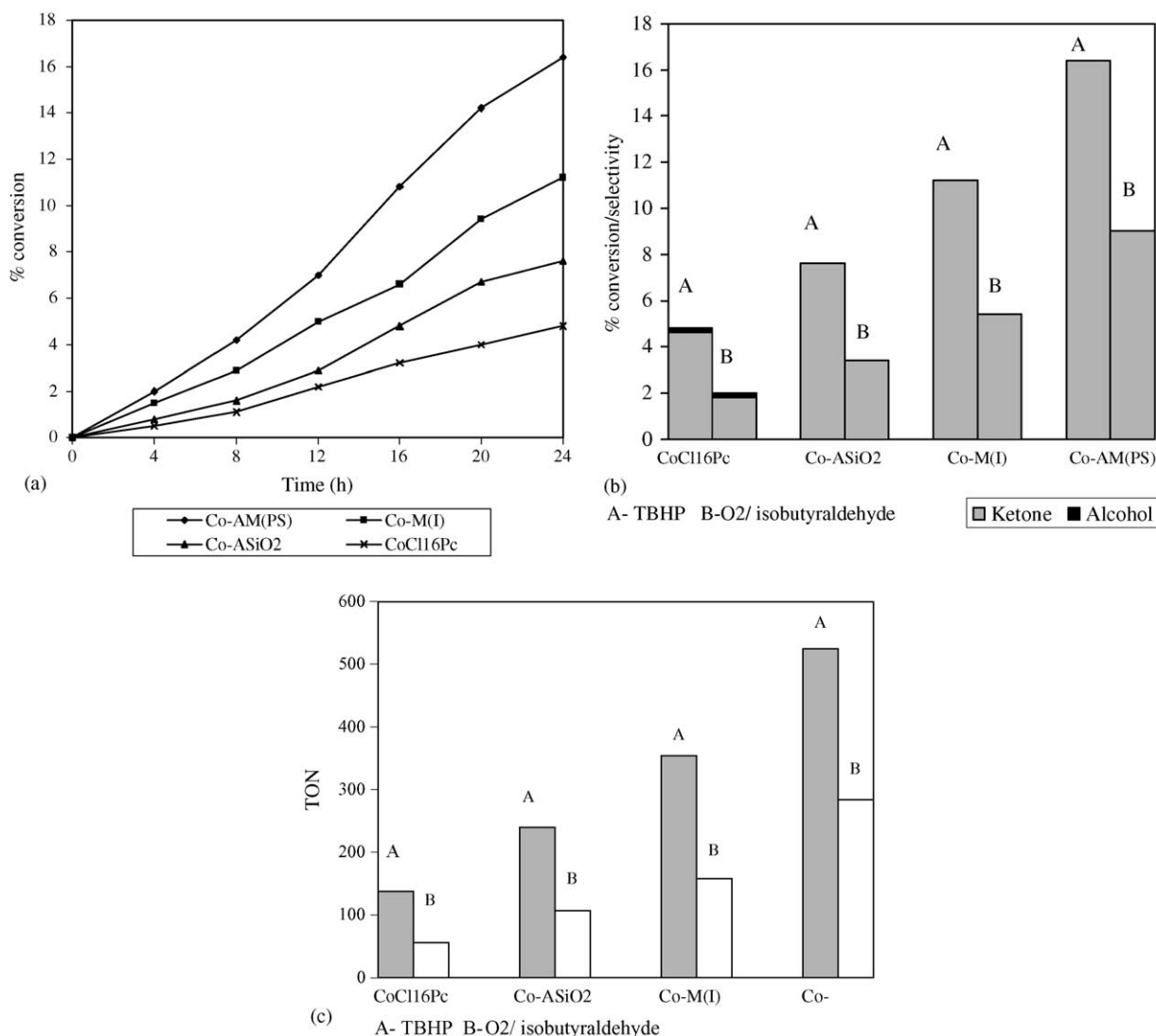
Fig. 7. (a) Kinetic study of *n*-decane oxidation using different CoCl$_{16}$Pc catalysts using TBHP as oxidant at 323 K. (b) Comparison of TBHP and O$_2$/isobutyraldehyde for *n*-decane oxidation using different CoCl$_{16}$Pc catalysts at 323 K. (c) Comparison of TON values for the different CoCl$_{16}$Pc catalysts: (A) TBHP and (B) O$_2$/isobutyraldehyde. TON = mole of product formed/mole of metal present in the catalyst/24 h.

AM(PS) showed a maximum conversion of 5.6 and 4.0% for TBHP and O$_2$/isobutyraldehyde, respectively, the conversions being 6.4% for TBHP and 4.6% for isobutyraldehyde over Co-AM(PS) at 298 K.

As mentioned earlier, Cu/Co-M(I) and Cu/Co-AM(PS) are the most active catalysts for both the oxidizing agents (Figs. 6(a) and 7(a)). When the two oxidizing agents are compared, the conversion of decane with TBHP is nearly double the conversion with O$_2$/isobutyraldehyde for all the catalysts at 323 K (Figs. 6(b) and 7(b)). Cu-AM(PS) shows 21.2% decane conversion for TBHP and 9.2% for O$_2$/isobutyraldehyde at 323 K. Similarly, Co-AM(PS) shows 16.4% conversion of decane for TBHP and 9.0% for O$_2$/isobutyraldehyde at the same temperature. Here also, the homolytic mechanism plays an important role in the oxidation reaction. But with both the oxidizing agents and both Cu/CoCl$_{16}$Pc complexes, a large decanone selectivity of ~95–97% (mixture of 2, 3, 4-decanones) with a small decanol selectivity

is observed, whereas for the complex grafted catalysts, ~100% selectivity is observed (Figs. 6(b) and 7(b)). The TON values at 323 K for the different catalysts for TBHP were: CuCl$_{16}$Pc, 116; Cu-ASiO$_2$, 234; Cu-M(I), 341 and Cu-AM(PS), 671 (Fig. 6(c)). Similarly, the TON values at the same temperature for O$_2$/isobutyraldehyde were: CuCl$_{16}$Pc, 59; Cu-ASiO$_2$, 101; Cu-M(I), 170 and Cu-AM(PS), 291 (Fig. 6(c)). For cobalt-containing catalysts, we observed a similar trend of TON values, the TON values for Co-AM(PS) being more than the other catalysts for both TBHP (TON = 525) and O$_2$/isobutyraldehyde (TON = 284) (Fig. 7(c)).

One should notice that the conversion of *n*-decane is more than that of cyclohexane over both the metal catalysts for both the oxidants. A similar behavior was observed in the case of titanium-containing siliceous catalysts used for the oxidation of alkanes [23]. This may be due to the differences in adsorption of *n*-alkane and cyclohexane over siliceous supports like MCM-41 [24].

Table 3
Oxidation of alkanes using (B) O_2/isobutyraldehyde and (C) O_2/benzaldehyde as co-oxidants over different catalysts of Cu/Co-Cl_{16}Pc

Catalyst	Oxidant	Cyclohexane			1-Decane		
		Conversion (%)	TON[a]	Selectivity[b] (mol%)	Conversion (%)	TON[a]	Selectivity[b] (mol%)
CuCl$_{16}$Pc (0.002 g)	B	1.6	47	37	2.0	59	98
	C	1.7	50	77	2.6	76	96
Cu-ASiO$_2$ (0.05 g)	B	2.2	70	36	3.2	101	~100
	C	2.8	88	66	3.8	120	~00
Cu-M(I) (0.05 g)	B	3.8	120	56	5.4	170	~100
	C	6.2	196	70	9.0	184	~100
Cu-AM(PS) (0.05 g)	B	6.2	196	60	9.2	291	~100
	C	9.4	297	68	15.4	487	~100
CoCl$_{16}$Pc (0.002 g)	B	2.2	62	41	2.0	56	98
	C	3.2	89	77	4.7	138	96
Co-ASiO$_2$ (0.05 g)	B	3.4	107	42	3.4	107	~100
	C	4.2	132	67	6.0	190	~100
Co-M(I) (0.05 g)	B	4.2	123	59	5.4	158	~100
	C	7.3	214	66	9.3	273	~100
Co-AM(PS) (0.05 g)	B	6.4	188	60	9.0	284	~100
	C	12.4	364	68	14.4	423	~100

Conditions: substrate = 5 mmoles; co-oxidant = 15 mmoles (1:3); solvent = acetonitrile 10 g; molecular oxygen 1 atm; temperature 323 K.
[a] TON = mole of product formed/mole of metal present in the catalyst/24 h.
[b] Selectivity for respective ketone.

3.7.3. Oxidation of alkanes using two different co-oxidation systems

Table 3 presents a comparative study of O_2/isobutyraldehyde with O_2/benzaldehyde as co-oxidants for the oxidation of alkanes under mild reaction conditions (323 K). Results show that, for both the oxidants, Cu/Co-AM(PS) is a better catalyst compared to the neat metal complex, Cu/Co-ASiO$_2$ and Cu/Co-M(I).

For the different catalysts of Cu/Co-Cl$_{16}$Pc, results of cyclohexane oxidation show that O_2/benzaldehyde gives ~1.5 times higher TON values compared to those for O_2/isobutyraldehyde (Table 3). This may be due to the higher resonance stability of the intermediate aromatic acyl peroxy radical in the case of benzaldehyde compared to isobutyraldehyde. Cu-AM(PS) gives 9.4% conversion of cyclohexane for O_2/benzaldehyde and 6.2% for O_2/isobutyraldehyde. Co-AM(PS) gives 12.4% cyclohexene conversion for O_2/benzaldehyde and 6.4 % for O_2/isobutyraldehyde at 323 K. The selectivity of cyclohexanone is also higher in the case of O_2/benzaldehyde as the oxidant; the cyclohexanol:cyclohexanone ratio is 1.0:2.0 compared to 1.0:1.5 for O_2/isobutyraldehyde.

Table 3 also presents the data for the oxidation of decane over each of the metal catalysts. It is again observed that Cu/Co-AM(PS) is the most active catalyst for the oxidation of decane for both the oxidants at 323 K. O_2/benzaldehyde giving more than 1.5 times higher decane conversion than O_2/isobutyraldehyde. For both the oxidants and for all the catalysts, the selectivity for decanone is large (more than 96%).

4. Conclusions

Planar complexes of copper and cobalt immobilized on a hydrophobic silica surface inside appropriately wide channels (as in MCM-41) are good catalysts for the oxidation of hydrocarbons under mild conditions using oxidants, such as TBHP and O_2/sacrificial aldehyde. Studies on the oxidation of cyclohexane and 1-decane with TBHP and O_2/aldehyde systems suggest that the differences in the conversions and product selectivity observed with the two oxidants may be attributed to mechanistic differences associated with the ease of formation of the free radical (alkyl/acyl species). O_2/benzaldehyde leads to a higher conversion of alkane compared to O_2/isobutyraldehyde. The resonance stability of the intermediate aromatic acyl peroxy radical is higher in the case of benzaldehyde than in the case of isobutyraldehyde. Also both TBHP and O_2/benzaldehyde possess comparable activity in oxidation reactions.

References

[1] J.T. Groves, W.J. Kruper, T.E. Nemo, R.S. Myers, J. Mol. Catal. 7 (1980) 169–177.
[2] P.C.H. Mitchell, Chem. Ind. 9 (1991) 308–311.
[3] U. Schuchardt, D. Cardoso, R. Sercheli, R. Pereira, R.S. de Cruz, M.C. Guerreiro, D. Mandelli, E.V. Spinace, E.L. Pires, Appl. Catal. A: Gen. 211 (2001) 1–17.
[4] A.B. Sorokin, A. Tuel, Catal. Today 57 (2000) 45–59.
[5] R. Raja, P. Ratnasamy, Catal. Lett. 48 (1997) 1–10.

[6] E. Armengol, A. Corma, V. Fornes, H. Garcia, J. Primo, Appl. Catal. A: Gen. 181 (1999) 305–312.

[7] J.W.M. Steeman, S. Kaarsemaker, P.J. Hoftyzer, Chem. Eng. Sci. 14 (1961) 139–149.

[8] C.-C. Guo, M.-F. Chu, Q. Liu, D.-C. Guo, X.-Q. Liu, Appl. Catal. A: Gen. 246 (2003) 303–309.

[9] A. Sakthivel, P. Selvam, J. Catal. 211 (2002) 134–143.

[10] N. Komiya, T. Naota, Y. Oda, S. Murahashi, J. Mol. Catal. A: Chem. 117 (1997) 21–37.

[11] S. Murahashi, Y. Oda, T. Naota, J. Am. Chem. Soc. 114 (1992) 7913–7914.

[12] P. Karandikar, M. Agashe, K. Vijayamohanan, A.J. Chandwadkar, Appl. Catal. A: Gen. 257 (2004) 133143.

[13] K. Chaudhari, T.K. Das, P.R. Rajmohanan, K. Lazar, S. Sivasanker, A.J. Chandwadkar, J. Catal. 183 (1999) 281–291.

[14] J.S. Beck, J.C. Vartuli, W.J. Roth, M.E. Leonowicz, C.T. Kresge, K.D. Schmidt, C.T.-W. Chu, D.H. Olson, E.W. Sheppard, S.B. McCullen, J.B. Higgins, J.L. Schlenker, J. Am. Chem. Soc. 114 (1992) 10834–10843.

[15] K.J. Balkus Jr., A.G. Gabrielov, S.L. Bell, F. Bedioui, L. Roue, J. Devynck, Inorg. Chem. 33 (1994) 67–71.

[16] H. Keypour, S. Salehzadeh, R.G. Pritchard, R.V. Parish, Inorg. Chem. 39 (2000) 5787–5790.

[17] M.P. Vinod, T.Kr. Das, A.J. Chandwadkar, K. Vijayamohanan, J.G. Chandwadkar, Mater. Chem. Phys. 58 (1999) 37–43.

[18] A. Wolberg, J. Manassen, J. Am. Chem. Soc. 92 (1970) 2982–2991.

[19] E.V. Rybak-Akimova, A.Y. Nazarenko, L. Chen, P.W. Krieger, A.M. Herrera, V.V. Tarasov, P. Robinson, Inorg. Chim. Acta 324 (2001) 1–15.

[20] N. Safari, F. Bahadoran, J. Mol. Catal. A: Chem. 171 (2001) 115–121.

[21] F.A. Chavez, C.V. Nguyen, M.M. Olmstead, P.K. Mascharak, Inorg. Chem. 35 (1996) 6282–6291.

[22] G. Russell, J. Am. Chem. Soc. 79 (1957) 3871–3877.

[23] R. Poladi, C.C. Landry, Microporous Mesoporous Mater. 52 (2002) 11–18.

[24] Y. Long, T. Xu, Y. Sun, W. Dong, Langmuir 14 (1998) 6173–6178.